## 1. KEY POINTS

From a structural dynamics perspective, the acceleration data for the five Dragon dockings that took place between GMT 2024-11-05 and 2026-02-14 yield the following key findings:

- **Context on SAMS System and Why the 6 Hz View** The Space Acceleration Measurement System (SAMS) sensors measure vibratory accelerations in the microgravity environment of the ISS with a nominal passband extending nominally to 200 Hz. While that full passband view is valuable for general vibratory characterization, it can obscure the salient features of a Dragon docking because higher-frequency, localized vibrations tend to dominate. In contrast, docking signatures are predominantly *low-frequency, global* structural responses that are more cleanly revealed in the lower-frequency structural-mode regime. Therefore, throughout this document we emphasize *6 Hz low-pass filtered* SAMS data to suppress localized high-frequency content, isolate the docking-driven response, then extract and present the most interpretable perspective for both structural dynamics and e.g. microgravity-fluids relevance.
- **Purpose of Dragon Dockings** SpaceX Dragon vehicles are used to transfer cargo and/or crew to and from the International Space Station (ISS).
- **"Station Quake"** ...okay, so not quite a quake, but still "ground shaking" as much as ISS structure is the ground. Imagine...the sudden impact of 2 massive spacecraft colliding (docking) while each is traveling at a ground track speed of around 17,500 miles/hour. In reality, during the final phase just before docking, the Dragon's trajectory (velocity magnitude and direction) is carefully choreographed to very closely match that of the gigantic space station other than a small delta in velocity along the orbital path to allow the Dragon to slowly close the gap. Mitigating factors for those concerned about the impact from the space station perspective: (1) the very large mass/inertia of the ISS weighing in at nearly a million pounds, (2) the carefully-crafted approach/relative trajectory, and (3) the "shock-absorbing" mating adapter. We will characterize and quantify the impact and acceleration signal/measurement features in this document.
- **Coordinate System** In this document – unless explicitly stated otherwise – we reference the body-fixed Space Station Analysis (SSA) coordinate system.
- **Advertised "Soft Capture" Time vs. SAMS-Measured "First Bump"** For the four Dragon dockings in 2024 and 2025, the as-flown timeline advertised *Soft Capture* time routinely occurred *after* the onset of the initial global structural response seen in low-pass (6 Hz) SAMS data ("first bump"), with offsets on the order of tens of minutes. However, the Crew-12 docking in 2026 is a clear counterexample: SAMS shows the "first bump" essentially coincident with (or slightly after) the reported soft-capture time. This break in the earlier 2024–2025 pattern indicates that the advertised soft-capture time should be treated as a reported, bookkeeping-type time stamp at the source where the timeline is produced, and not as a reliable proxy for the earliest disturbance onset measured and observed via SAMS data.
- **Port-Dependent Signatures:** The events shown include two Node 2 Forward (N2F) and three Node 2 Zenith (N2Z) dockings. These distinct port geometries produce *distinctly different* low-frequency acceleration signatures, while remaining closely *internally consistent* within each port type.

## 2. INTRODUCTION

On occasion, to transfer cargo and/or crew, a SpaceX Dragon vehicle is required to dock with the International Space Station (ISS). This document seeks to characterize the impact of five such docking events from 2024, 2025, and 2026.

Figure 1 (page 4) is an annotated artist rendering that identifies the two Node 2 docking ports discussed in this report: **N2Z** (Node 2 Zenith), the upper port in the figure, and **N2F** (Node 2 Forward), the forward port shown with a Cargo Dragon docked. While not called out in the rendering, an essential element in the interface is the *docking adapter* (ring-like hardware at the port) that provides the standardized mechanical interface used during approach and capture, and helps manage relative-motion energy during the capture/settling sequence.

Table 1. Five Dragon Docking Events from 2024, 2025, and 2026

| Vehicle | Port | Date | Soft Capture | SAMS First Bump | Delta (Minutes) |
|---|---|---|---|---|---|
| SpX-31 | N2F | 2024-11-05 | 15:15:00 | 14:52:25 | 22.6 |
| Ax-4 | N2Z | 2025-06-26 | 11:00:00 | 10:32:02 | 28.0 |
| Crew-11 | N2Z | 2025-08-02 | 07:00:00 | 06:27:07 | 32.9 |
| SpX-33 | N2F | 2025-08-25 | 11:30:00 | 11:05:45 | 24.3 |
| Crew-12 | N2Z | 2026-02-14 | 20:15:00 | 20:16:00 | -1.0 |

Table 1 above lists the five Dragon dockings analyzed. The columns are:

**Vehicle** Short mission/vehicle identifier (e.g., SpX-31 = SpaceX-31).

**Port** Node 2 docking port: **N2F** = Node 2 Forward, **N2Z** = Node 2 Zenith.

**Date** Docking date (YYYY-MM-DD).

**Soft Capture** as-flown timeline advertised Soft Capture time (HH:MM:SS). These times are drawn from an external as-flown activity/timeline source and should be treated as a reported bookkeeping time stamp at the source (not a direct measurement of the earliest structural response).

**SAMS First Bump** Data-driven onset time (HH:MM:SS) defined as the first clear, large low-frequency acceleration excursion seen in the 6 Hz low-pass filtered per-axis time histories, occurring near the reported soft-capture time window, and in the axis/direction implied by the destination port (e.g., for N2Z we expect an initial onset primarily in the $+Z$ axis).

**Delta (Minutes)** Time offset between Soft Capture and First Bump, computed as $\Delta t = t_{\text{Soft Capture}} - t_{\text{First Bump}}$, expressed in minutes.

Throughout, we use acceleration measurements from the SAMS sensor head `121f03` mounted in the US Lab (LAB1O1). Although Dragon docking disturbances are predominantly *global* structural events—and qualitatively similar signatures are observed in Columbus and JEM—the measured response does exhibit localized differences based on sensor head location. Such spatial variation is expected for a distributed structure, reflecting local mounting conditions and proximity to the excitation and dominant structural load paths. That being said, you can reference the data shown here as representative of what one would expect in the US Lab locale for such Dragon vehicle dockings.

## 3. QUALIFY

This section provides a mostly qualitative analysis and description of 2 types of Dragon dockings: (1) three dockings to the Node 2 Zenith port (N2Z), and (2) two dockings to the Node 2 Forward port (N2F).

The 2 Hz, 70-minute color spectrograms in Figures 2 and 3 (plus the two-sensor view for Crew-12 in Figures 4 and 5) both show a narrow frequency slice of the acceleration spectrum (zoomed in on structural mode and crew activity regime) during Dragon dockings to the Node 2 Zenith port. The most salient feature besides "first bump" are structural excitation and ringout/decay down at about 0.17 Hz. A consistent feature throughout all five Dragon dockings, in fact.

The two color spectrograms in Figures 6 and 7 show the same narrow frequency slice of the acceleration spectrum, but now during Dragon dockings to the Node 2 Forward port.

All five Dragon docking spectrograms show these 2 primary features: (1) initial impulse ("first bump"), and (2) excitation of 0.17 Hz structural mode. We will get a better look at these in the Quantify section below.

## 4. QUANTIFY

Note that ancillary labeling on the figures in this section reference “inverted-sams” data. This stems from a wiring polarity issue intrinsic to SAMS sensor head data. Whenever directionality is a key feature for acceleration events, we must first invert on a per-axis basis to address this issue.

To better visualize the Dragon dockings’ impact on the structural dynamics regime, we provide 6 annotated, per-axis acceleration versus time figures in Figures 8 through 13 (including the two-sensor view for Crew-12 in Figures 10 and 11) starting on page 11.

The first 4 figures were dockings at the Node 2 Zenith port with these similar, prominent features: (1) “first bump” in the $+Z$-axis direction, and (2) excitation and ringout at about 0.17 Hz. We do see some $Y$-axis excitation, but to a much lesser extent than the $Z$- and $X$-axes.

For the Crew-12 docking on 2026-02-14 (Node 2 Zenith), we include the same two views from two distributed SAMS heads: 121f03 at LAB1O1 (Figures 4 and 10) and es20 at LAB1S2 (MSG) (Figures 5 and 11). This side-by-side inclusion is intended to (i) confirm the global nature of the docking impulse and low-frequency ringout, and (ii) highlight any location-dependent differences in per-axis response and relative amplitude.

For the 121f03 view (Figure 10), the X-axis time history additionally overlays a 0.4 Hz low-pass filtered (LPF) trace (black) on the 6 Hz LPF data (dim gray background) to remove some of the other structural response (frequencies) and better highlight the duration of the ~0.17 Hz ringout on that axis (~90 s).

*Crew-12 Two-Sensor View (121f03 and es20)*

For the Crew-12 docking (GMT 2026-02-14, N2Z), we also include measurements from SAMS sensor head `es20` located in the US Lab at `LAB1S2` (MSG). Both sensor heads (`121f03` and `es20`) indicate the same “first bump” time reported in Table 1, and the dominant “first bump” axis/direction is consistent with the other N2Z dockings (i.e., a prominent onset primarily in the $+Z$ axis).

The next 2 figures referenced in this section were dockings at the Node 2 Forward port with these similar, prominent features: (1) "first bump" in the $-X$-axis direction, and (2) excitation and ringout at about 0.17 Hz. For these, we do see short-lived impact on all three axes, but primarily along the $X$-axis.

Figure 15 (page 14) provides a side-by-side comparison of the 6 Hz low-pass filtered data (left) and the unfiltered, as-measured data (right). While the filtered plot clearly isolates the structural impact of the Dragon docking, the unfiltered plot illustrates the presence of high-frequency components that obscure signal features at this scale. Notably, the peak-to-peak (pk2pk) scales differ by a factor of approximately 30, highlighting the significant "noise" reduction achieved through low-pass filtering.

## 5. CONCLUSION

This report used SAMS acceleration measurements to characterize five SpaceX Dragon docking events spanning GMT 2024-11-05 to 2026-02-14. The primary sensor head was `121f03` mounted in the US Lab (LAB1O1); for the 2026 Crew-12 docking we also include a second sensor head, `es20`, in the US Lab at `LAB1S2` (MSG), to provide a two-location view of the same event. To emphasize the global, low-frequency structural response most relevant to vehicle-level dynamics (and to e.g. microgravity-fluids investigations), the analysis focused on 6 Hz low-pass filtered data and a structural-mode frequency slice.

Across all five dockings, two repeatable features dominate the response: (1) a short impulsive onset ("first bump") marking the earliest clear global structural excitation, followed by (2) a consistent ring-down near ∼0.17 Hz lasting on the order of ∼40–60 seconds. While the overall appearance is consistent, the docking port shapes the directionality of the initial response: the three Node 2 Zenith (N2Z) dockings show a prominent first-bump signature primarily in the $+Z$ axis, whereas the two Node 2 Forward (N2F) dockings show the first bump primarily in the $-X$ axis, with smaller responses on the other axes.

An important timing takeaway is that the advertised *Soft Capture* time is not a reliable proxy for the SAMS-observed "first bump" onset. In the four dockings from 2024 and 2025, the reported soft-capture time lags the SAMS "first bump" by ∼20–33 minutes; the Crew-12 docking in 2026 is a clear counterexample, with the SAMS "first bump" essentially coincident with (or slightly after) the reported soft-capture time. This break in pattern suggests the soft-capture time should be treated as a reported bookkeeping-type time stamp at the source where the as-flown timeline is produced, rather than as a consistent physical marker of the earliest global structural excitation. For conservative disturbance windows, the SAMS-observed "first bump" remains the appropriate earliest-onset indicator of docking-driven global response.

Finally, the comparison of 6 Hz low-pass filtered data to the full as-measured passband highlights why a low-frequency view is operationally necessary: in the full 200 Hz passband, higher-frequency content typically would mask docking-specific low-frequency effects. For experimenters and analysts, the recommended workflow is to (i) identify the first bump in the low-frequency view, (ii) quantify the subsequent ∼0.17 Hz ring-down envelope, and (iii) use port type (N2Z vs N2F) as a consistent guide to the expected dominant axis and qualitative signature.

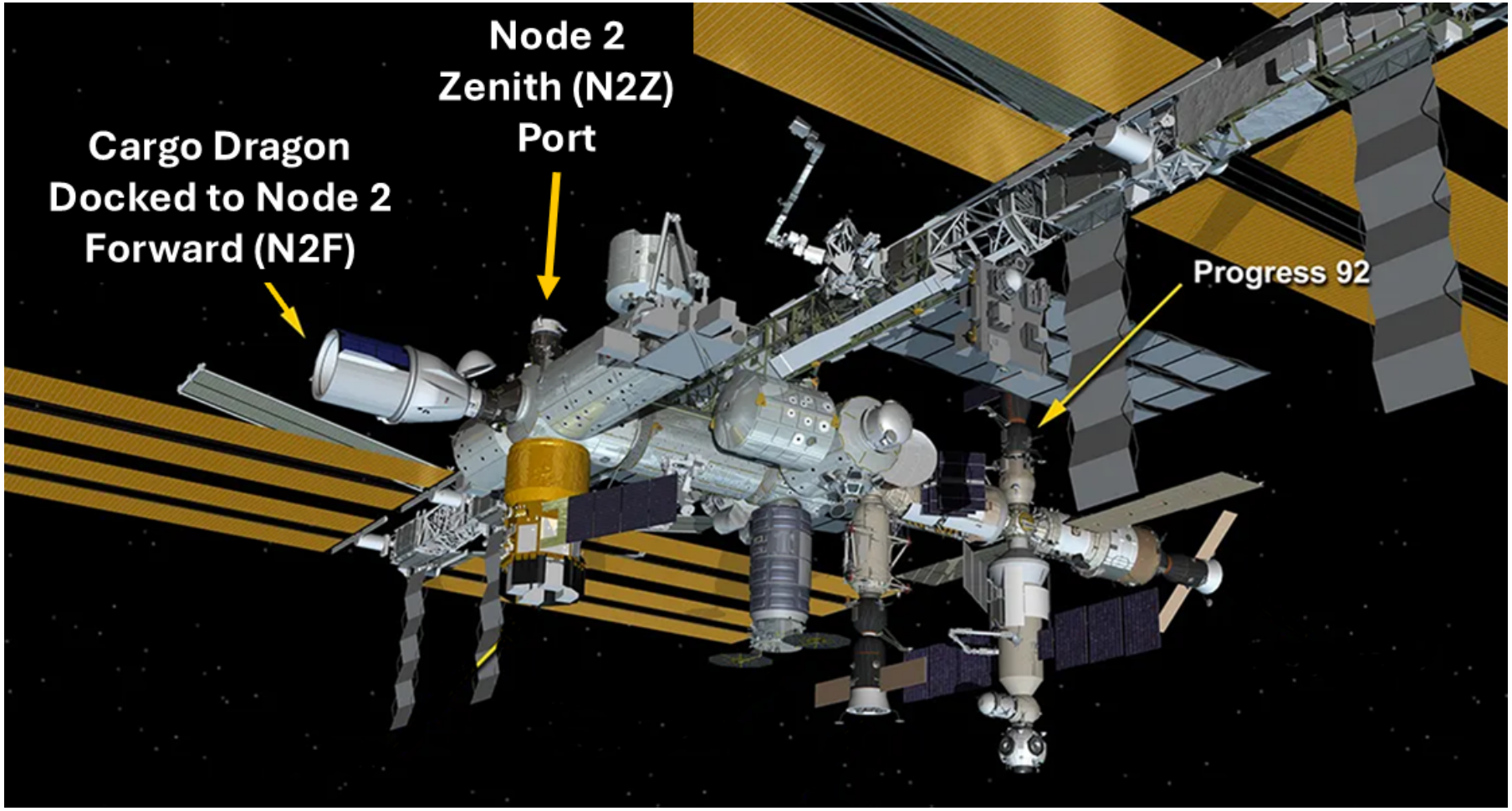


Fig. 1: Node 2 Docking Ports.

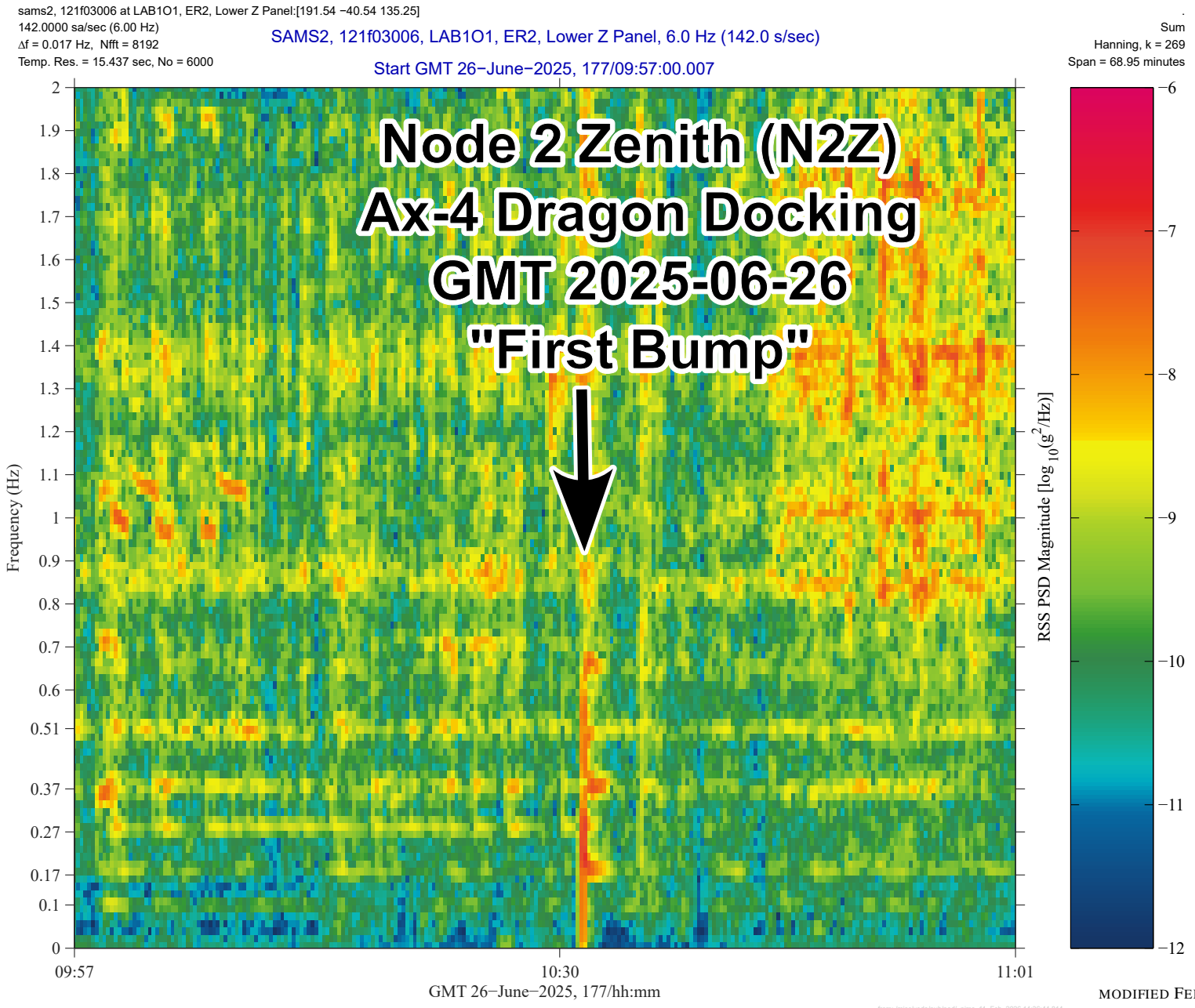




Fig. 2: Dragon Docking, Node 2 Zenith Port, GMT 2025-06-26.

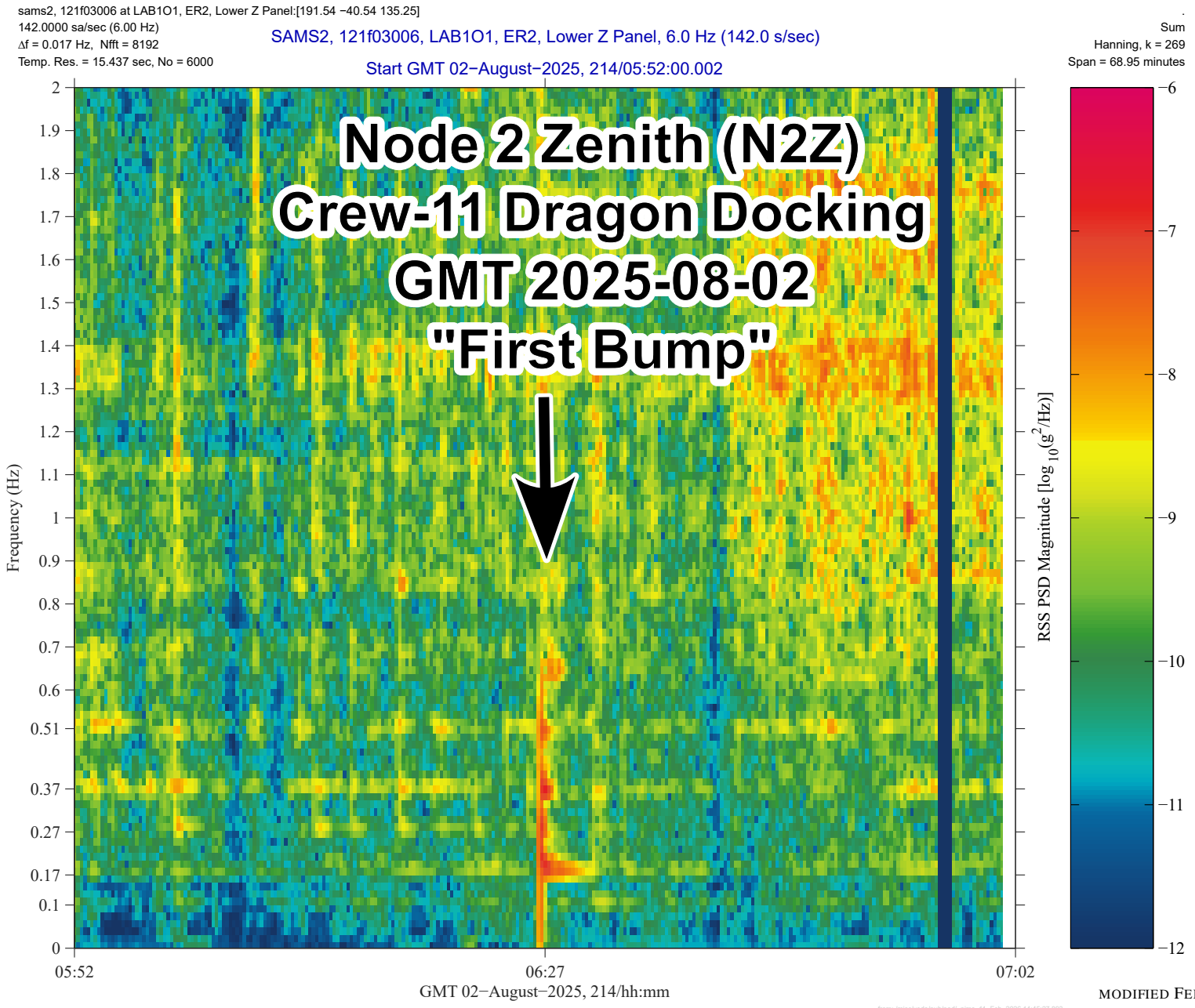




Fig. 3: Dragon Docking, Node 2 Zenith Port, GMT 2025-08-02.

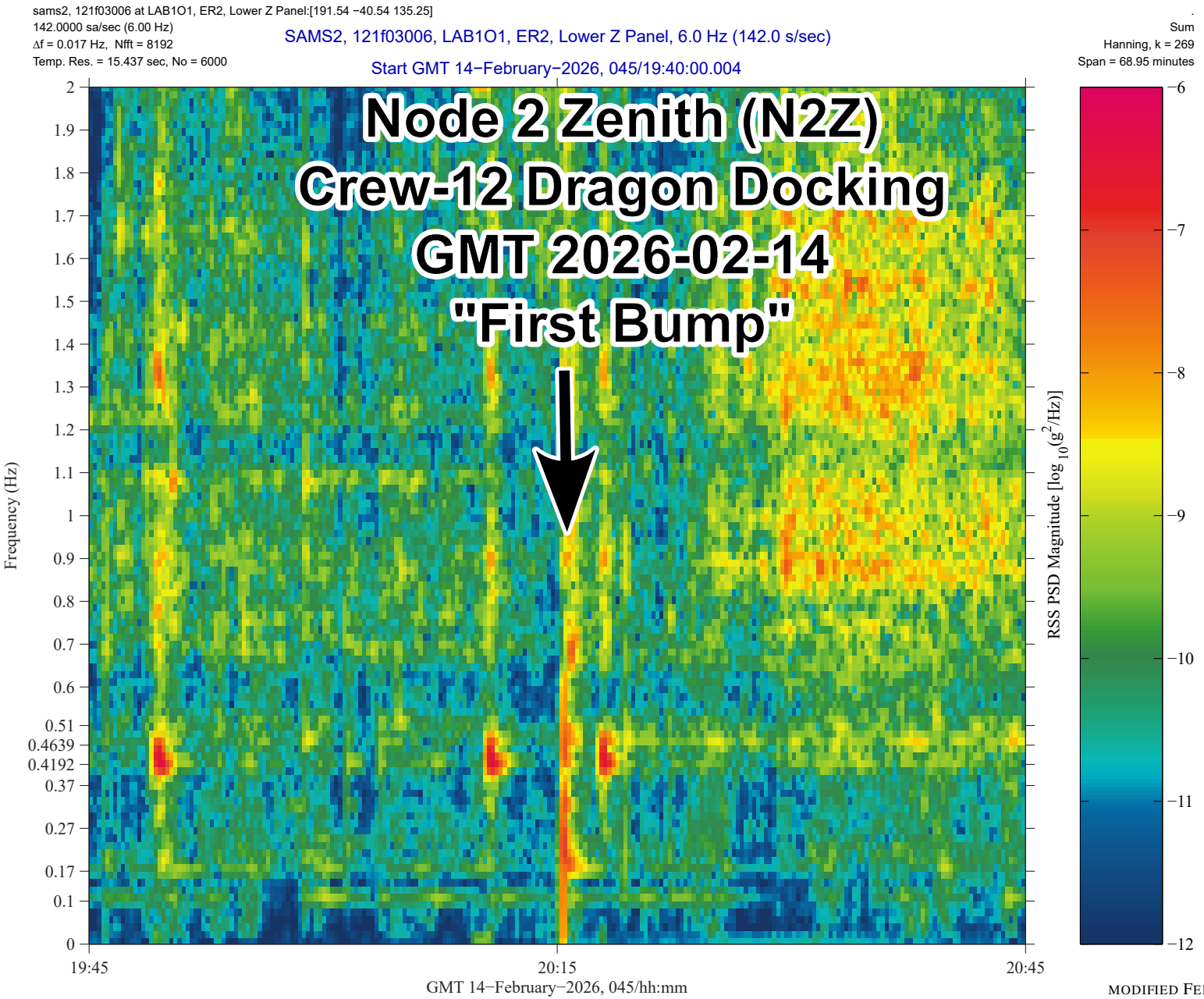




Fig. 4: Dragon Docking, Node 2 Zenith Port (Crew-12), GMT 2026-02-14; SAMS 121f03 at LAB1O1.

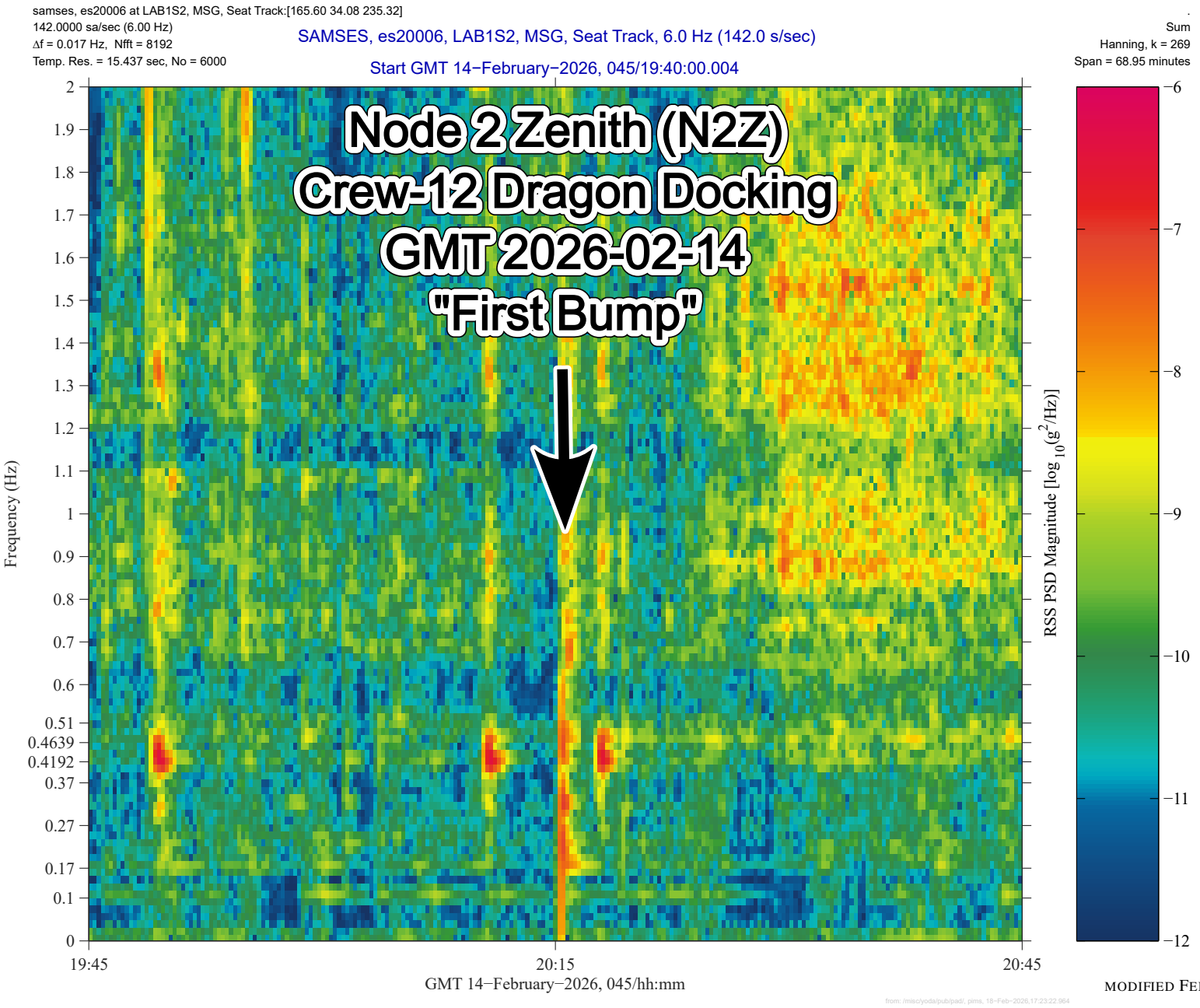




Fig. 5: Dragon Docking, Node 2 Zenith Port (Crew-12), GMT 2026-02-14; SAMS es20 at LAB1S2 (MSG).

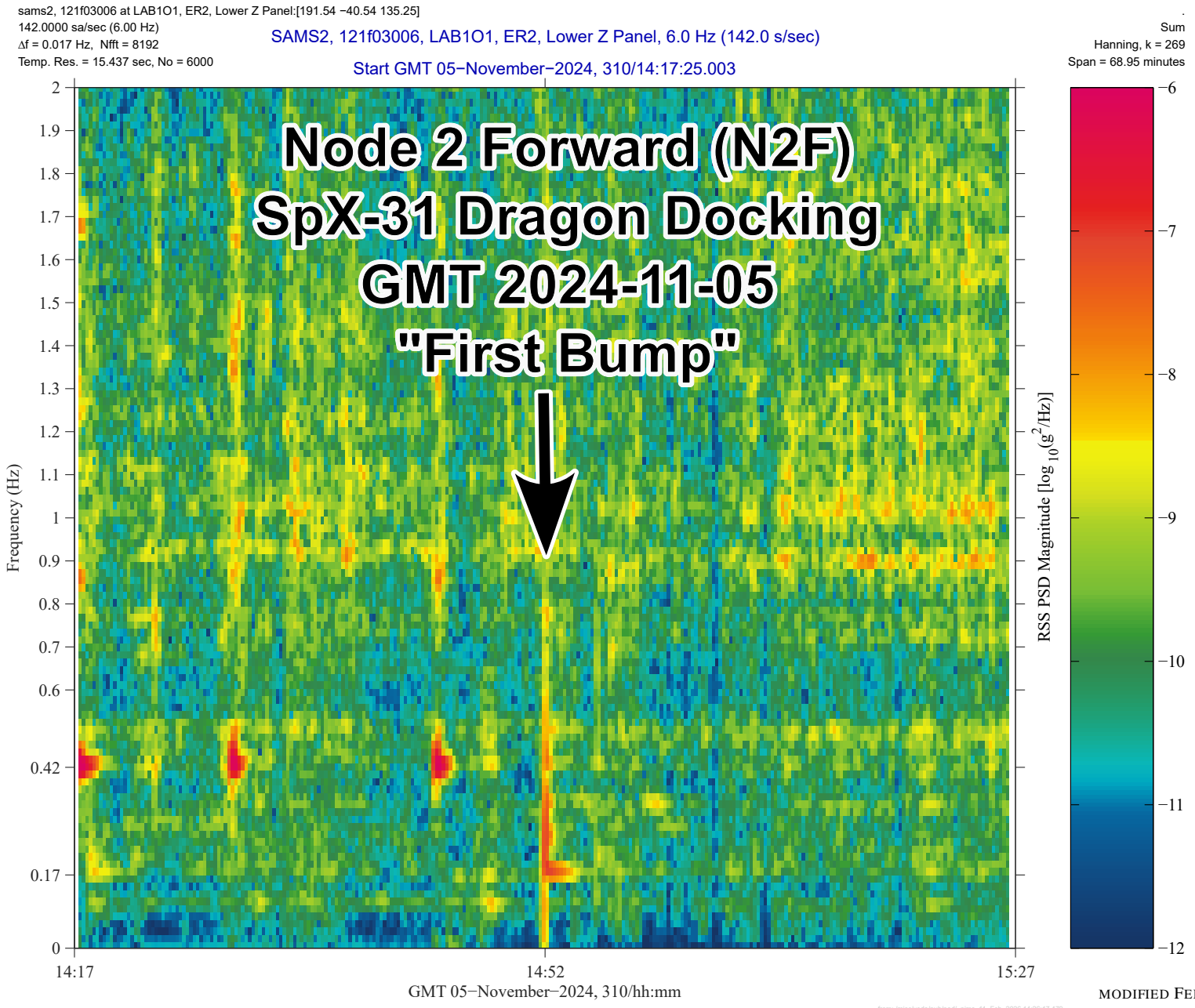




Fig. 6: Dragon Docking, Node 2 Forward Port, GMT 2024-11-05.

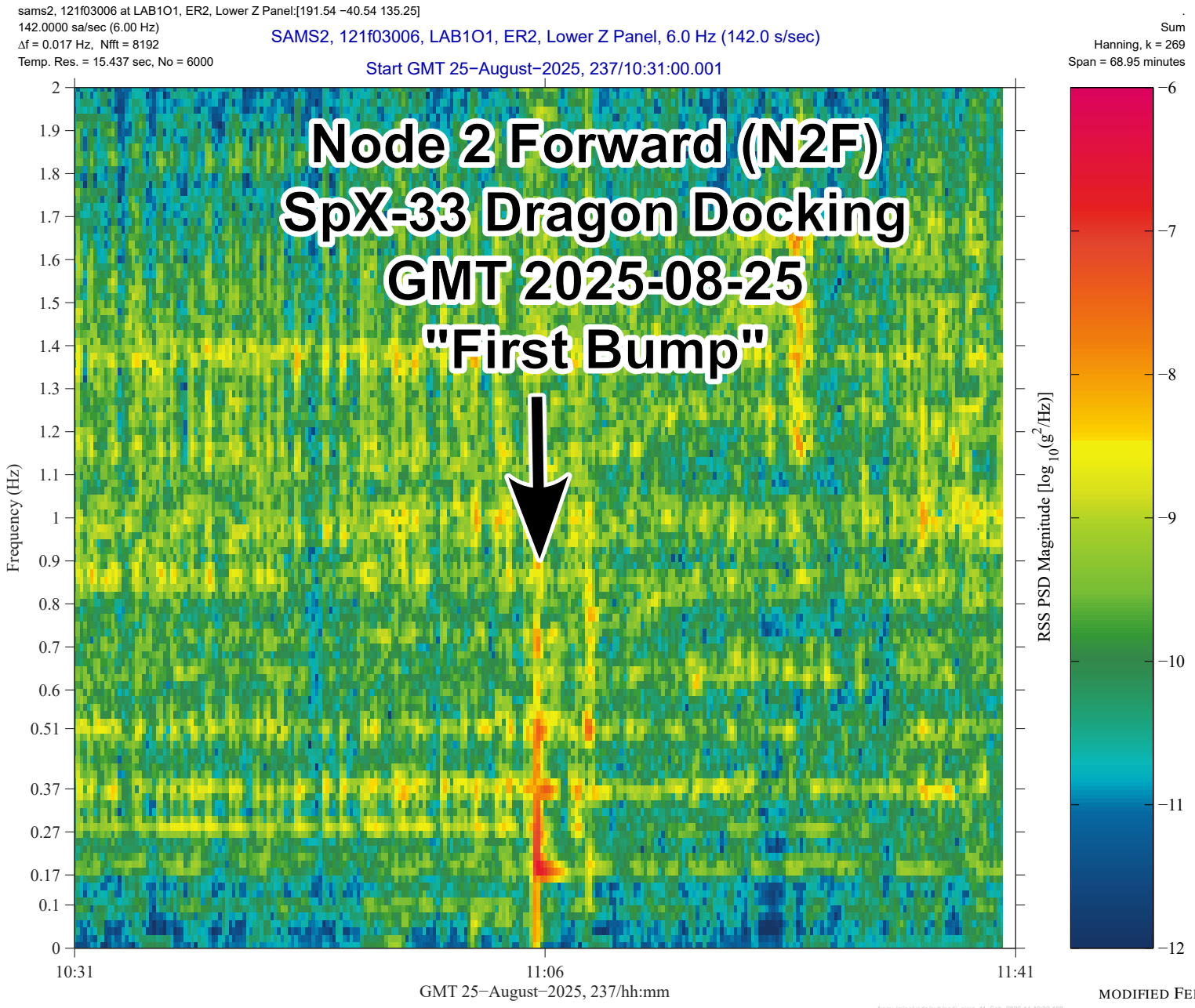




Fig. 7: Dragon Docking, Node 2 Forward Port, GMT 2025-08-25.

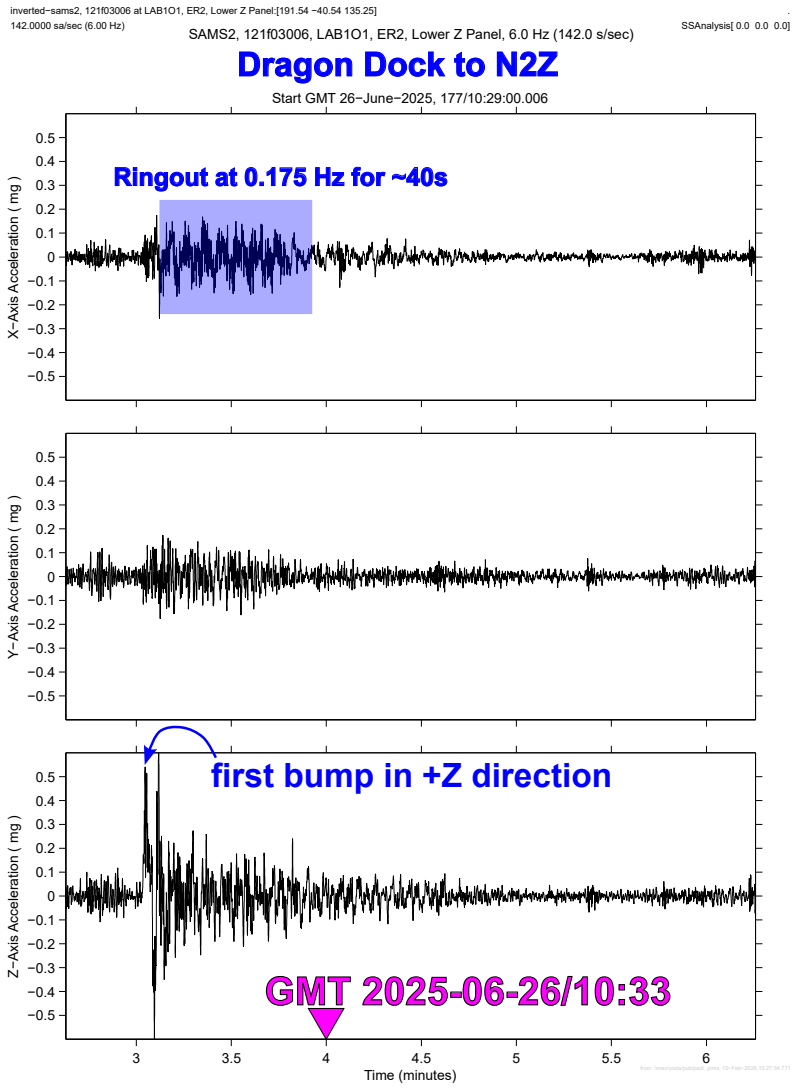


Fig. 8: ~3.6-Min, 6 Hz $a_{xyz}(t)$ via SAMS 121f03 Sensor at LAB1O1 (ER2).

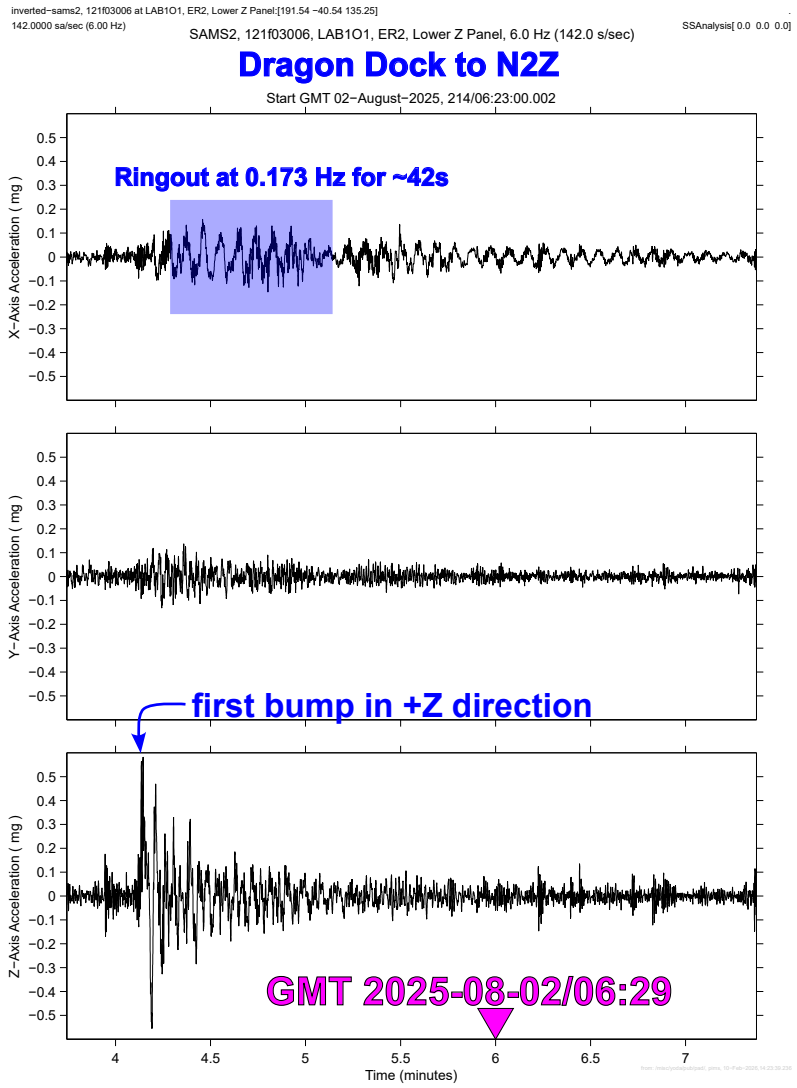


Fig. 9: ~3.6-Min, 6 Hz $a_{xyz}(t)$ via SAMS 121f03 Sensor at LAB1O1 (ER2).

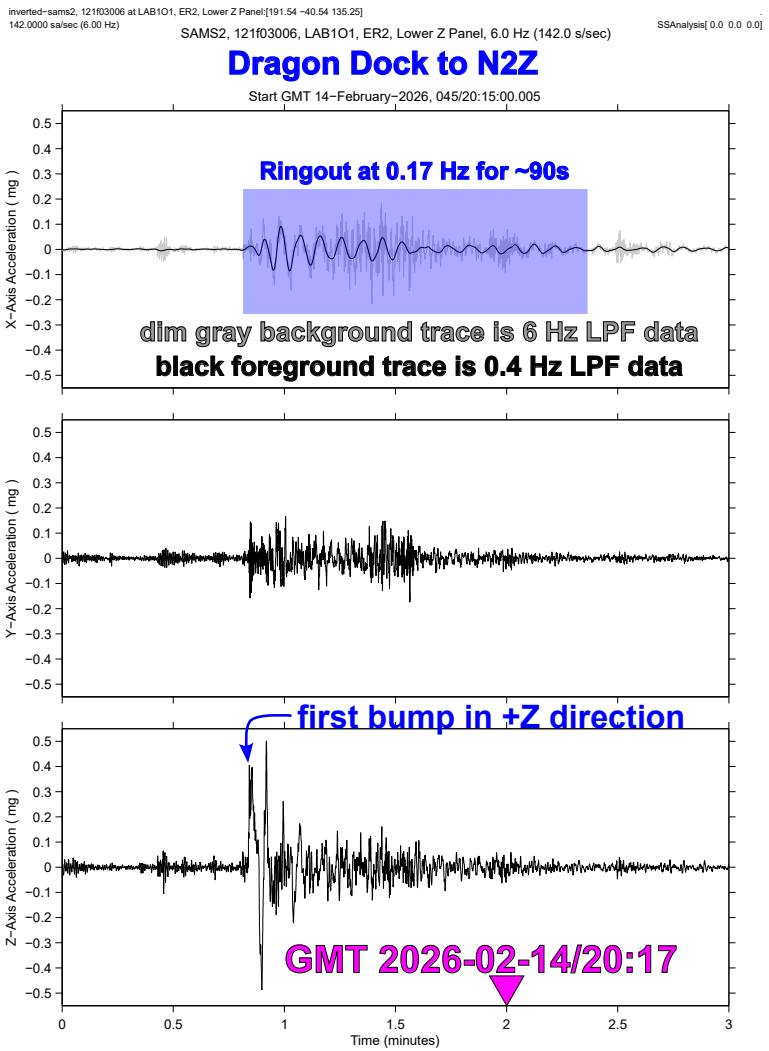


Fig. 10: 3-Min, 6 Hz $a_{xyz}(t)$, SAMS 121f03 Sensor at LAB1O1 (Crew-12, N2Z). **Top subplot (X-axis only):** dim gray background trace = 6 Hz data; black foreground trace = 0.4 Hz low-pass filtered data.

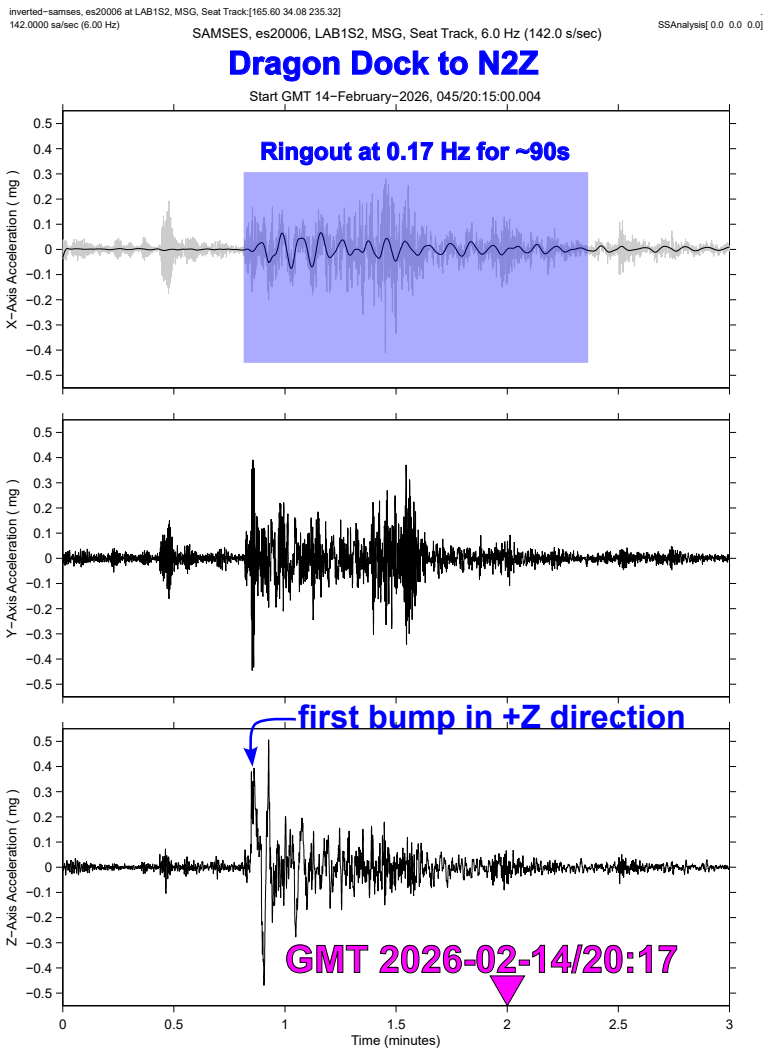


Fig. 11: 3-Min, 6 Hz $a_{xyz}(t)$, SAMS es20 Sensor at LAB1S2 (Crew-12, N2Z). **Top subplot (X-axis only):** dim gray background trace = 6 Hz data; black foreground trace = 0.4 Hz low-pass filtered data.

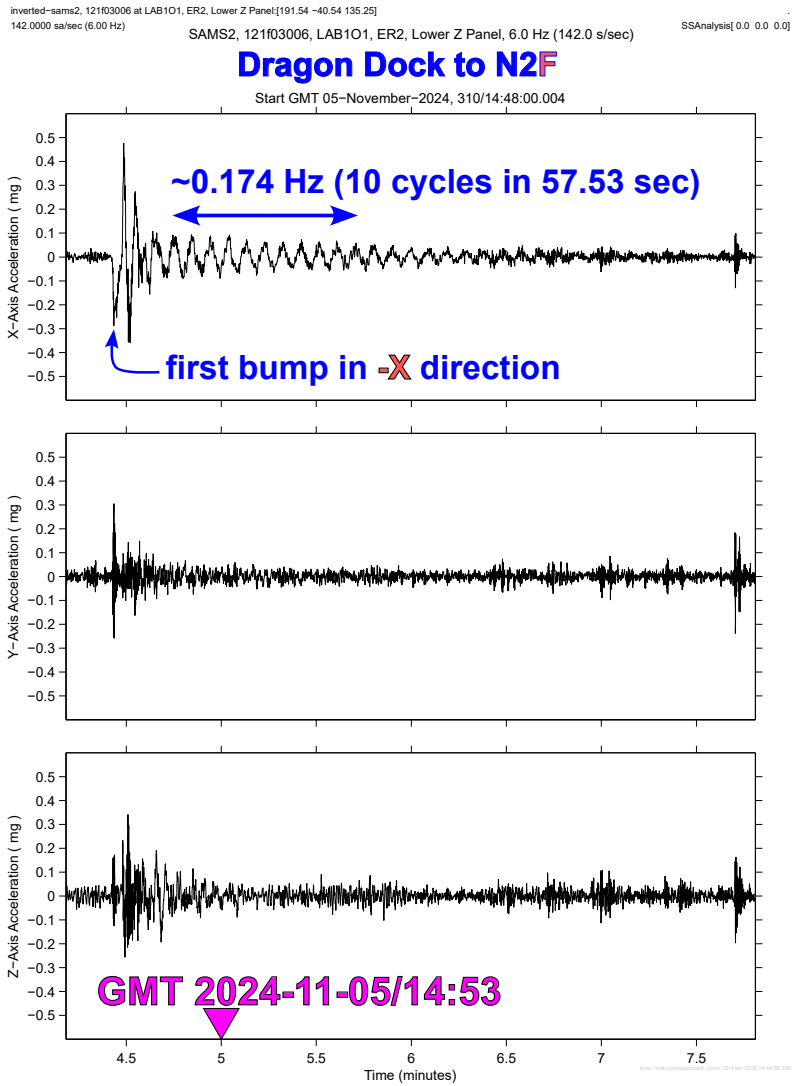


Fig. 12: ~3.6-Min, 6 Hz $a_{xyz}(t)$ via SAMS 121f03 Sensor at LAB1O1 (ER2).

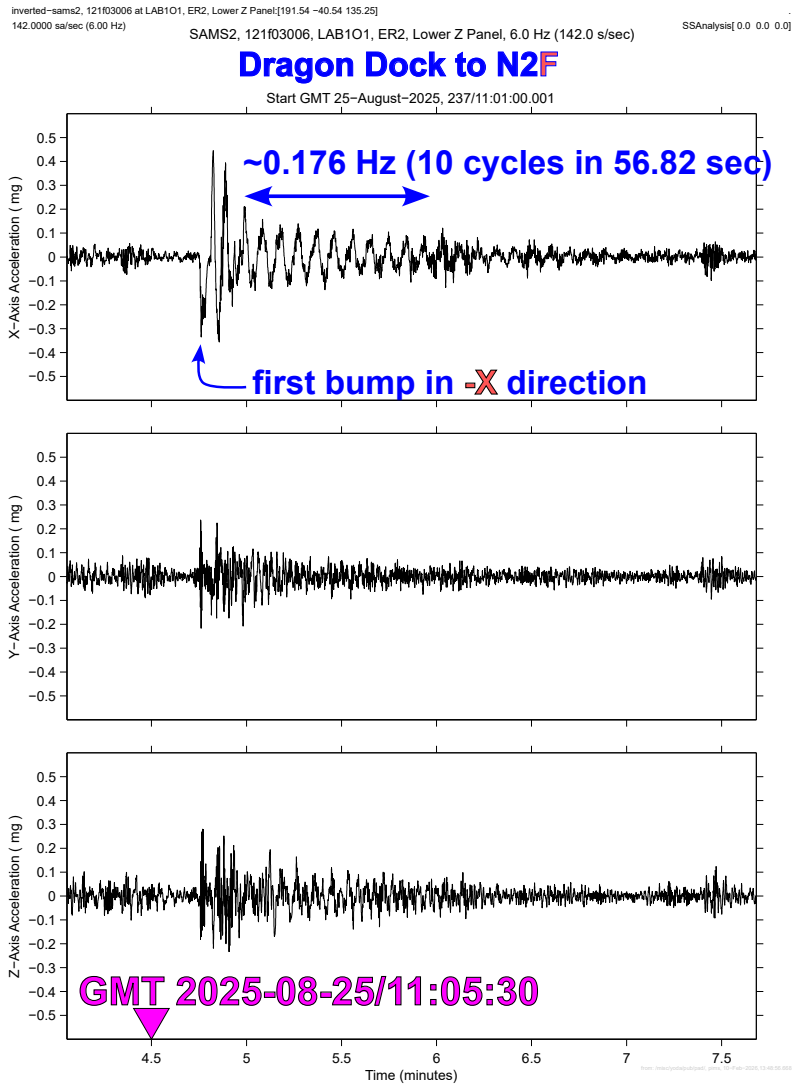


Fig. 13: ~3.6-Min, 6 Hz $a_{xyz}(t)$ via SAMS 121f03 Sensor at LAB1O1 (ER2).

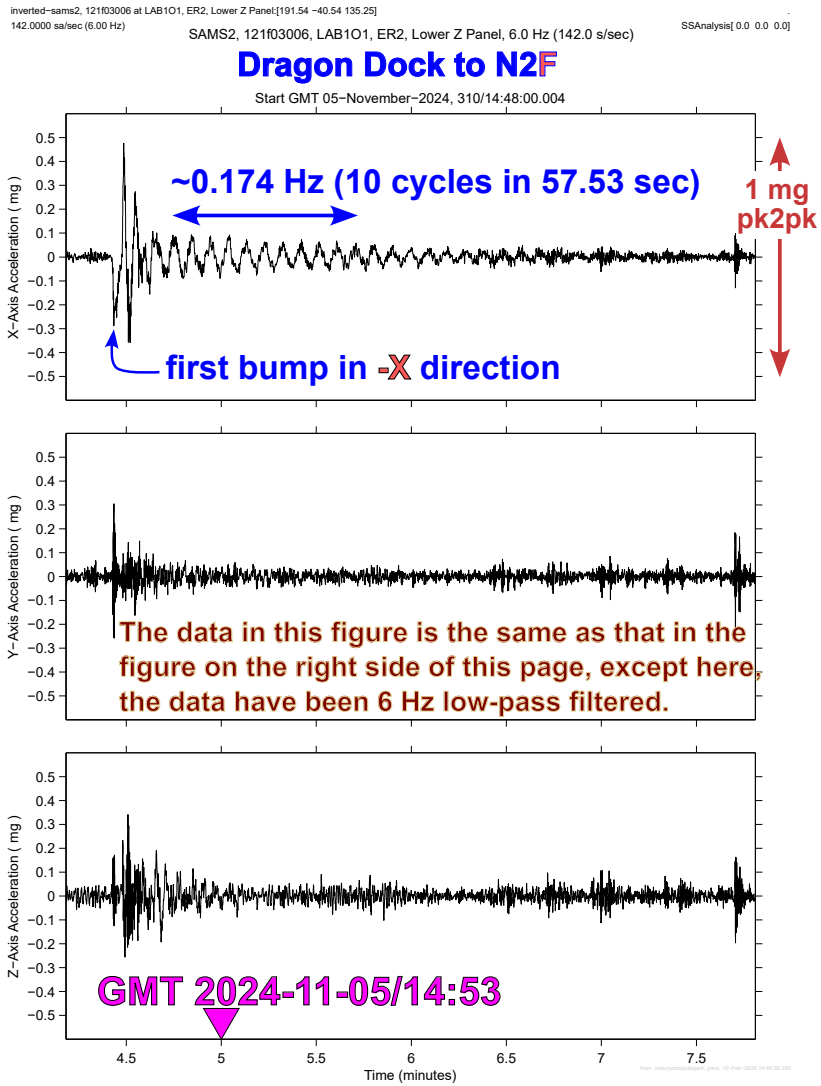


Fig. 14: ~3.6-Min, 6 Hz $a_{xyz}(t)$ via SAMS 121f03 Sensor at LAB1O1 (ER2).

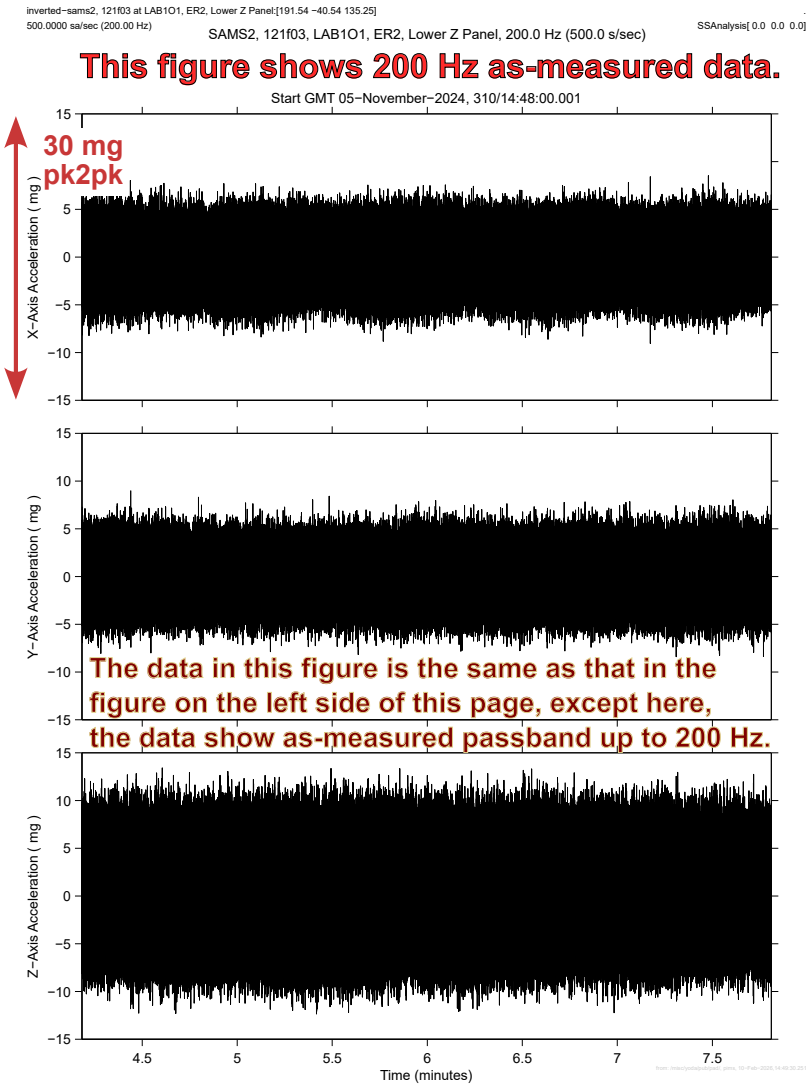


Fig. 15: ~3.6-Min, 200 Hz $a_{xyz}(t)$ via SAMS 121f03 Sensor at LAB1O1 (ER2).